



ELSEVIER



CrossMark



Automatically Adapted Perfectly Matched Layers for Problems with High Contrast Materials Properties

J. Alvarez-Aramberri¹, D. Pardo², and H. Barucq³

¹ University of the Basque Country (UPV/EHU), Bilbao, Spain, Inria team-project Magique-3D, and LMA UMR 5142 UPPA, Pau, France
julen.alvarez.aramberri@gmail.com

² Department of Applied Mathematics, Statistics, and Operational Research at the University of the Basque Country (UPV/EHU), and IKERBASQUE, Basque Foundation for Science, Bilbao, Spain
dzubiaur@gmail.com

³ EPC Magique-3D, Inria, LMA, University of Pau, F64013 Pau, France
helene.barucq@inria.fr

Abstract

For the simulation of wave propagation problems, it is necessary to truncate the computational domain. Perfectly Matched Layers are often employed for that purpose, especially in high contrast layered materials where absorbing boundary conditions are difficult to design. In here, we define a Perfectly Matched Layer that automatically adjusts its parameters without any user interaction. The user only has to indicate the desired decay in the surrounding layer. With this Perfectly Matched Layer, we show that even in the most complex scenarios where the material contrast properties are as high as sixteen orders of magnitude, we do not introduce numerical reflections when truncating the domain, thus, obtaining accurate solutions.

Keywords:

1 Introduction

When applying *hp*-adaptivity for the Finite Element Method (FEM) [6] in open region problems the computational domain has to be truncated. In particular, it is crucial for wave equations problems, which typically exhibit oscillating solutions with slow decay. If we attempt to truncate the computational domain by reducing the domain size via a change of coordinates from an infinite domain to a finite one, the solution oscillates more and more when approaching the boundary, and these oscillations are hardly reproduced by numerical methods. If we just truncate the domain without using carefully designed boundary conditions, then we observe non-physical reflections coming from the boundary.

In 1994, in a seminal paper of Berenger [2], Perfectly Matched Layers (PML) were proposed in an electromagnetic context as an artificial layer intended to reduce reflections from the

boundary of a truncated computational domain. A new interpretation of PMLs was introduced by Teixeira and Chew [5, 16], where also in the context of electromagnetic phenomena, they interpreted a PML as a change of coordinates into the complex plane.

PMLs transform propagating and evanescent waves into exponentially fast decaying evanescent waves. Because of the high attenuation of the waves into the PML region, we can impose some boundary conditions (BC) (typically homogeneous Dirichlet BC) on the outer part of the PML without introducing appreciable reflections. For a further understanding and for a recent review of the state of the art of this truncation technique, we refer to [3] and [9].

When implementing PMLs, one has to *select* the decay profile of the wave into the PML region. Selecting a profile that produces arbitrarily small reflections implies that the solution also decays arbitrarily fast, which produces a “boundary layer” and strong gradients in the region. Thus, while a low decay produces incoming waves reflected from the boundary, an excessive decay requires a very fine grid. To find an equilibrium between a fast and a slow decay, it is necessary to properly adjust the PML parameters, which is usually tricky since they depend on the problem itself. Moreover, when we have a layered material with high contrasts on the material properties, this selection of the parameters is even more challenging.

The main contribution of this work is to provide a method to automatically adjust the PML parameters, even in the most complex scenarios where the material contrast properties among neighbouring materials are as high as sixteen orders of magnitude. These type of scenarios often appear in geophysical electromagnetic (EM) applications that involve both, air and ground. We show using a two dimensional (2D) magnetotelluric (MT) [4, 17, 14] application that the proposed PML produces an appropriate decay of the solution in the air and in the subsurface without introducing spurious reflections, and thus, it provides accurate solutions.

The present work is organized as follows. In Section 2 we define the mathematical problem to be solved. Section 3 describes the formulation of the PML and how the parameters to be tuned in the PML are automatically adjusted. Numerical results based on the MT problem are illustrated in Section 4 and Section 5 is devoted to the conclusions.

2 Model Problem

In this work, we study this automatically adapted PML in context of MTs.

2.1 MT Method

The MT is a passive EM exploration technique intended to estimate the resistivity distribution, and therefore provide an *image* of the subsurface on scales varying from few meters to hundreds of kilometers [18]. MT measurements can be described by Maxwell’s equations, with the source located at the ionosphere. In particular, when the electrical field depends only upon two spatial variables (x, z) , we can derive two uncoupled modes from Maxwell’s equations, namely, *Transverse Electric* (TE), which involves (E_y, H_x, H_z) electric and magnetic field components, and *Transverse Magnetic* (TM), which involves (H_y, E_x, E_z) .

We focus on the *E-Formulation*, where the equation for the y component can be expressed as

$$-\mu^{-1}\Delta E_y - \mathbf{k}^2 E_y = -j\omega J_y^{imp}, \quad (1)$$

where $\mathbf{k}^2 = \omega^2\varepsilon - j\omega\boldsymbol{\sigma}$, E_y is the y -component of the electric field driven by an impressed prescribed density current J_y^{imp} , ω is the angular frequency and $\boldsymbol{\sigma}$ (a diagonal second rank tensor) stands for the conductivity of the media. For the range of frequencies involving the MT

problem, the electrical permittivity ε and the magnetic permeability μ can be assumed to be that of the vacuum (ε_0 and μ_0 respectively).

Using an *hp*-Finite Element Method [6], we compute the electric field E_y . Our aim is to obtain the impedance and/or the apparent resistivity, two suitable physical magnitudes to perform the inversion. To do so, the magnetic field is obtained from Maxwell's equations, namely:

$$H_x = \frac{1}{j\omega\mu} \frac{\partial E_y}{\partial z}. \tag{2}$$

The impedance Z_{yx} and the apparent resistivity ρ_a are then computed using the following formulas:

$$Z_{yx} = \frac{E_y}{H_x} \quad \rho_a = \frac{|Z_{yx}|}{\omega\mu}. \tag{3}$$

2.2 Variational Formulation

For the sake of simplicity in the notation, we omit the y subscript from E_y and J_y^{imp} . Thus, to obtain the corresponding variational formulation we multiply equation (1) by the complex conjugate of a test function $F \in V(\Omega)$, where $V(\Omega) = H_{\Gamma_D}^1(\Omega) = \{F \in L^2(\Omega) : F|_{\Gamma_D} = 0, \nabla F \in L^2(\Omega)\}$ is the space of admissible test functions. Then, we integrate by parts and incorporate the homogeneous Dirichlet BC (the ones considered in the present work) over $\Gamma_D = \partial\Omega$, and we obtain that

$$\left\{ \begin{array}{l} \text{Find } E \in E^D + V(\Omega), \text{ such that:} \\ \int_{\Omega} (\nabla \bar{F})^T \mu^{-1} \nabla E - \int_{\Omega} \bar{F} \mathbf{k}^2 E = -j\omega \int_{\Omega} \bar{F} J^{imp} \quad \forall F \in V(\Omega), \end{array} \right. \tag{4}$$

where E^D is a lift (typically $E^D = 0$) of the essential boundary condition data denoted with the same symbol. With the *state* scalar-valued solution function E , we compute $L^i(E)$, a linear and continuous functional [12, 11] in E associated to the i -th receiver and defined as:

$$L^i(E) = \frac{1}{|\Omega_{R^i}|} \int_{\Omega_{R^i}} E d\Omega, \tag{5}$$

where Ω_{R^i} is the domain occupied by the i -th receiver.

3 PML Formulation

Chew and Weedon [5] showed that a PML can be understood as a complex-coordinate stretching of Maxwell's equations. With this interpretation, the PML is simply an analytic continuation of the governing equations into the complex plane (see also [15]).

3.1 Variational Formulation in an Arbitrary System of Coordinates

Let the Cartesian coordinate system $\mathbf{x} = (x, z) = (x_1, x_2)$ be the reference system of coordinates. Given an arbitrary system of coordinates $\boldsymbol{\zeta} = (\zeta_1, \zeta_2)$, we define our change of coordinates by $\mathbf{x} = \boldsymbol{\psi}(\boldsymbol{\zeta})$ and we denote the Jacobian matrix and its determinant by \mathcal{J} and $\det(\mathcal{J})$, respectively. The change of coordinates is assumed to be an injective differentiable function with

continuous partial derivatives and nonzero determinant at any point. The corresponding variational formulation for the TE mode, in the new system of coordinates, can be obtained as follows.

Let $E = E(\mathbf{x})$ and $F = F(\mathbf{x})$ be an arbitrary scalar-valued functions. Since they are analytical functions, we extend them to the complex plane. We denote $\tilde{E} := E \circ \boldsymbol{\psi} = \tilde{E}(\zeta)$ and $\tilde{F} := F \circ \boldsymbol{\psi} = \tilde{F}(\zeta)$. Additionally, we define $\tilde{\mu} := \mu \circ \boldsymbol{\psi}$, $\tilde{\mathbf{k}} := \mathbf{k} \circ \boldsymbol{\psi}$, $\tilde{J}^{imp} := J^{imp} \circ \boldsymbol{\psi}$, $\tilde{\Omega} := \Omega \circ \boldsymbol{\psi}$, and $\tilde{\Gamma}_D := \Gamma_D \circ \boldsymbol{\psi}$.

Multiplying equation (1) by the complex conjugate of a test function \tilde{F} , integrating by parts, and incorporating the homogeneous Dirichlet BC over $\tilde{\Gamma}_D = \partial\tilde{\Omega}$, we obtain that:

$$\begin{aligned} \int_{\tilde{\Omega}} (\nabla^\zeta \tilde{F})^T \tilde{\mu}^{-1} \nabla^\zeta \tilde{E} \, d\tilde{\Omega} &= \int_{\Omega} \left((\mathcal{J}^{-1})^T \nabla \tilde{F} \right)^T \mu^{-1} (\mathcal{J}^{-1})^T \nabla E \, \det(\mathcal{J}) \, d\Omega = \\ &= \int_{\Omega} (\nabla \tilde{F})^T \mathcal{J}^{-1} \mu^{-1} (\mathcal{J}^{-1})^T \nabla E \, \det(\mathcal{J}) \, d\Omega, \\ \int_{\tilde{\Omega}} \tilde{F} \tilde{\mathbf{k}}^2 \tilde{E} \, d\tilde{\Omega} &= \int_{\Omega} \tilde{F} \mathbf{k}^2 E \, \det(\mathcal{J}) \, d\Omega, \\ \int_{\tilde{\Omega}} \tilde{F} \tilde{J}^{imp} \tilde{E} \, d\tilde{\Omega} &= \int_{\Omega} \tilde{F} J^{imp} \, \det(\mathcal{J}) \, d\Omega, \end{aligned} \tag{6}$$

where we use the chain rule,

$$\nabla^\zeta \tilde{E} = \sum_{i,n}^2 \frac{\partial \tilde{E}}{\partial x_i} \frac{\partial x_i}{\partial \zeta_n} = (\mathcal{J}^{-1})^T \nabla E. \tag{7}$$

Following the ideas of [19] concerning the inclusion of metric-dependent variables within material coefficients, we define the following functions:

$$\begin{aligned} \boldsymbol{\mu}_{NEW}^{-1} &= \mathcal{J}^{-1} \mu^{-1} (\mathcal{J}^{-1})^T \det(\mathcal{J}), \\ \mathbf{k}_{NEW}^2 &= \mathbf{k}^2 \det(\mathcal{J}), \\ J_{NEW}^{imp} &= J^{imp} \det(\mathcal{J}). \end{aligned} \tag{8}$$

The new source and material tensors incorporate the information about the change of coordinates. Thus, the variational formulation can be expressed in terms of an arbitrary system of coordinates by simply considering the new source and materials. The new variational formulation, in the new system of coordinates is:

$$\left\{ \begin{array}{l} \text{Find } E \in E^D + \tilde{V}(\Omega), \text{ such that:} \\ \int_{\Omega} (\nabla \tilde{F})^T \boldsymbol{\mu}_{NEW}^{-1} \nabla E \, d\Omega - \int_{\Omega} \tilde{F} \mathbf{k}_{NEW}^2 E \, d\Omega = \int_{\Omega} \tilde{F} J_{NEW}^{imp} \, d\Omega, \quad \forall F \in \tilde{V}(\Omega), \end{array} \right. \tag{9}$$

where $\tilde{V}(\Omega) = \tilde{H}_{\Gamma_D}^1(\Omega) = \{E \in L^2(\Omega) : E|_{\Gamma_D} = 0, (\mathcal{J}^{-1})^T \nabla E \in \mathbf{L}^2(\Omega)\}$.

3.2 Definition of the PML

We define a general one dimensional change of variables, in the positive direction of the i -th coordinate, of the type

$$\zeta_i(x_i) = \int_0^{x_i} h(\eta) d\eta, \quad \text{for } i = 1, 2. \tag{10}$$

The case corresponding to the negative direction is defined analogously. The Jacobian and its determinant are given by

$$\mathcal{J} = \begin{pmatrix} \frac{\partial \zeta_1}{\partial x_1} & \frac{\partial \zeta_1}{\partial x_2} \\ \frac{\partial \zeta_2}{\partial x_1} & \frac{\partial \zeta_2}{\partial x_2} \end{pmatrix} = \begin{pmatrix} h(x_1) & 0 \\ 0 & h(x_2) \end{pmatrix} \quad \text{and} \quad \det(\mathcal{J}) = h(x_1)h(x_2). \quad (11)$$

Thus, μ_{NEW}^{-1} is given by:

$$\mu_{NEW}^{-1} = \begin{pmatrix} \mu_0^{-1} \frac{h(x_2)}{h(x_1)} & 0 \\ 0 & \mu_0^{-1} \frac{h(x_1)}{h(x_2)} \end{pmatrix}. \quad (12)$$

3.3 Automatic Adjustment of PML Parameters

Given the general change of coordinates (10), we select

$$h(x_i) = \begin{cases} 1, & x_i < x_i^a \\ \phi_i \in \mathbb{C}, & x_i \in [x_i^a, x_i^b], \end{cases} \quad (13)$$

where $[x_i^a, x_i^b]$ define the position of the PML in the positive direction of the i -th coordinate.

If the space far from the region of interest is linear, homogeneous, and the problem is time-harmonic, the radiating solution for some wave equation is a sum of plane waves, and may be decomposed into functions of the form of $e^{-j\kappa x_i}$ (see [8]), where $\kappa = \sqrt{\omega^2 \mu \epsilon - j\omega \mu \sigma}$ is the wave number and x_i is the direction of propagation of the wave.

We consider the worse scenario, that is, a plane wave traveling perpendicularly to the PML towards the positive direction of the x_i variable (an analogous analysis can be done for the negative direction). Then, the solution in the PML region for the new variable is given by

$$E(\zeta(x_i)) = e^{-j\kappa \zeta(x_i)} = e^{-j\kappa \phi_i x_i}. \quad (14)$$

Our aim is to make the solution to vanish in the PML region without introducing reflections. Therefore, we define the decay factor α , which measures the decay of the solution from x_i^a to x_i^b , as

$$\alpha := \frac{E(x_i^b)}{E(x_i^a)} = e^{-j\kappa \phi_i (x_i^b - x_i^a)}. \quad (15)$$

Then,

$$\log(\alpha) = -j\kappa \phi_i (x_i^b - x_i^a) \quad (16)$$

and finally, we select

$$\phi_i = j \frac{\log(\alpha)}{\kappa (x_i^b - x_i^a)}. \quad (17)$$

Remark. Notice that with this formula we obtain an automatic adjustment of the PML parameters. The user does not have to take care about the formation material within each area, even

if they change abruptly. On the other hand, different size for the PML can be considered in each side of each variable. The only user interaction is to define the desired decay into the PML region, i.e., α . Then, ϕ_i is automatically computed guaranteeing a decay in the outer part of the PML according to the selected α .

4 Numerical Results

This automatically adjusted PML is suitable for a variety of problems where the material contrast properties among neighbouring materials are large. In particular, we will study its impact into our MT model problem.

4.1 Model Problem

We assume a horizontally layered earth model where some 2D inhomogeneities may appear. The TE mode is driven by the impressed electric density current $\mathbf{J}^{imp} = \omega \hat{\mathbf{y}}$. We model the source as an infinitely long (in x and y directions) volumetric rectangular surface located at the ionosphere. This allows us to treat the electromagnetic fields as plane waves that propagate in the vertical direction towards the Earth's surface [17].

The physical problem is illustrated in Figure 1. The computational domain in consideration, of 2500×130 km. consist of air and a layered media (eventually with a scatter) for modelling the subsurface formation. The horizontal dimension corresponds to the x spatial variable (with zero at the center), and the vertical to the z (with zero on the surface). The physical domain is surrounded by a PML. The relative permittivity and permeability are the same in all materials, and equal to one. The receivers are located at the Earth's surface and are represented with red crosses, while the source, located at the ionosphere is represented with the dark blue rectangle. When the media is only 1D dependent (invariant in x), the solution along the surface is constant (x and y independent), and therefore, it is sufficient to consider only one receiver. However, when 2D inhomogeneities are considered, we are interested in having the solution at different positions. We consider four different formation of the subsurface described in Table 1. The

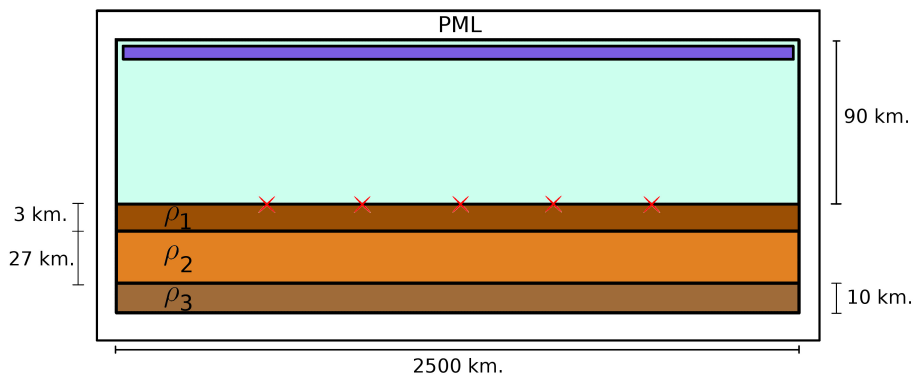


Figure 1: Model problem.

exact solution for a 1D layered media is known (see for example [13, 7]). For numerical results, we calculate the electric field solving (1). In a layered media problem we use a multigoal-oriented hp -FEM [10, 1], which ensures accurate solutions at all receivers.

	ρ_1	ρ_2	ρ_3
Model 1	1	1	1
Model 2	1	10	3
Model 3	1	10	10
Model 4	1	100	3

Table 1: Different models for the formation of the subsurface. Resistivities are given in Ohm-m.

4.2 Validation of the Solution

We first ensure that our automatically adapted PML provides accurate solutions for a range of frequencies. We consider a 5 km. PML in all directions. The mesh in each direction of the PML region is depicted in Figure 2. The number of elements into the PML region represents 15.5% of the total amount of elements. We define a decay factor of $\alpha = 10^{-5}$, ensuring that

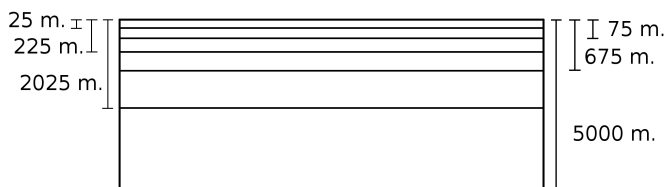


Figure 2: Horizontal layers of the FEM mesh in an arbitrary direction into the PML region.

the wave decays sufficiently fast when arriving to the boundary of the domain. In Figure 3, we represent the apparent resistivity against the frequency for the exact (left) and numerical (right) solutions. We observe a good agreement between both solutions. Figure 4 displays the error for the whole range of frequencies. Our PML provides always relative errors below 1.5%, which is a superb accuracy for these type of simulations. Finally, we consider Model 4

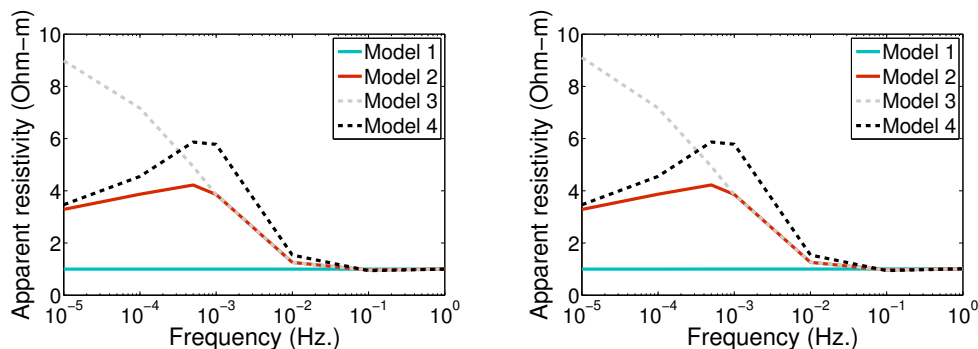


Figure 3: Apparent resistivity against frequency for the exact (left) and numerical (right) solutions.

problem for $\omega = 10^{-4}$ Hz. In Figure 5 we display the logarithm of the module of the impedance i.e., $\log(|Z_{yx}|)$, along all sides of the computational domain. We show that the PML behaves properly everywhere, with a smooth decay for the solution and without introducing numerical reflections even in the areas with high contrast between material properties. Panels (a) and (b)

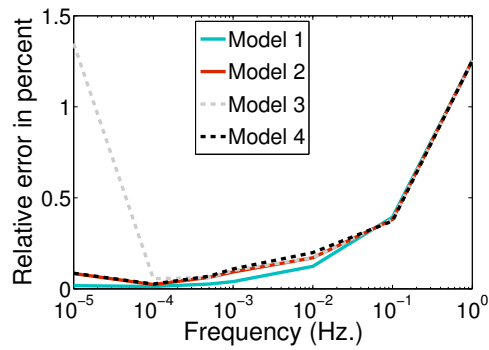


Figure 4: Relative error for different subsurface formations for a range of frequencies.

correspond to the intersection between air and ground. There, the contrast between resistivities is about sixteen orders of magnitude and even in this scenario, the decay is appropriate.

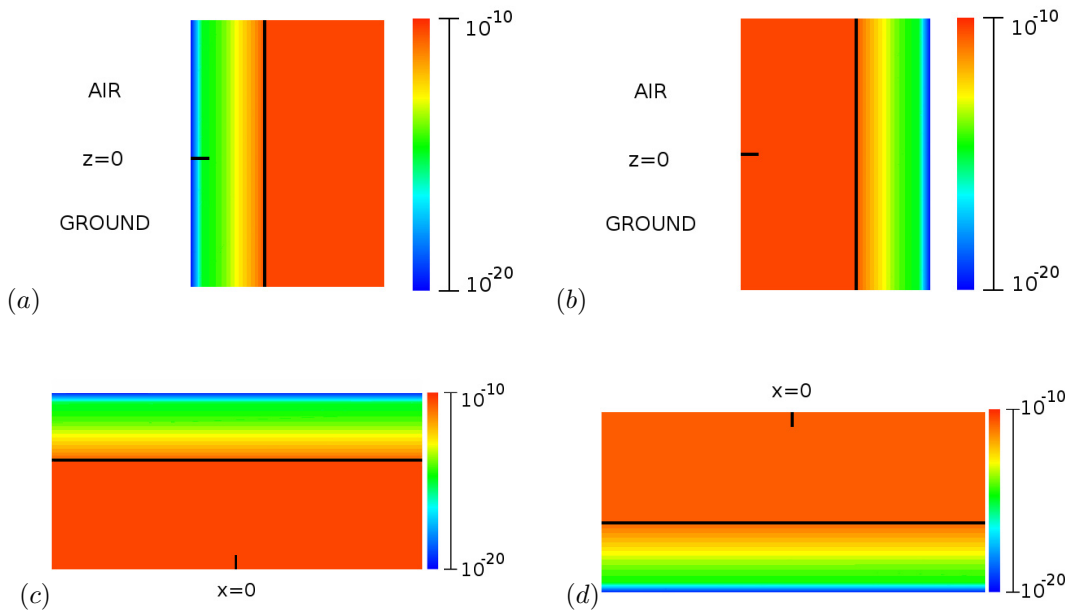


Figure 5: $\log(|Z_{yx}|)$ corresponding to Model 4, with a 5 km. PML and $\alpha = 10^{-5}$. Panel (a) corresponds to the left side of the domain. (b), (c), and (d) correspond to the right, top and bottom parts of the domain, respectively. The black line indicates the region where the PML starts.

4.3 Formation with a Target/Scatterer

We consider a 2D inhomogeneity located at the center of the domain inside the layer corresponding to ρ_2 . The horizontal length of this target is 10 km. and we denote its resistivity with

ρ_4 . In Figure 6 (left) we consider the problem called Target in Table 2 and we represent the apparent resistivity at different distances from the center of the domain for a range of frequencies. Position 1 corresponds to the center of the domain, which coincides with the center of the target. The effect of the target is more notorious there, and as expected, we measure higher resistivities at this point than elsewhere.

Our capacity to detect the target lies on our capability to capture the inhomogeneities in the solution. This fact depends on the considered frequency. For example, for $\omega = 10^{-1}$ we cannot detect any inhomogeneity because all our measurements are almost the same everywhere. On the other hand, if our aim is to detect the target, $\omega = 10^{-3}$ Hz. is the more appropriate frequency to consider. For this frequency, we represent in Figure 6 (right) the solution along the surface for the three different problems described in Table 2. In there, we appreciate how our solution is sensitive to the presence of the target. In particular, we observe that the solution is more affected when the receiver is closer to the target, as expected.

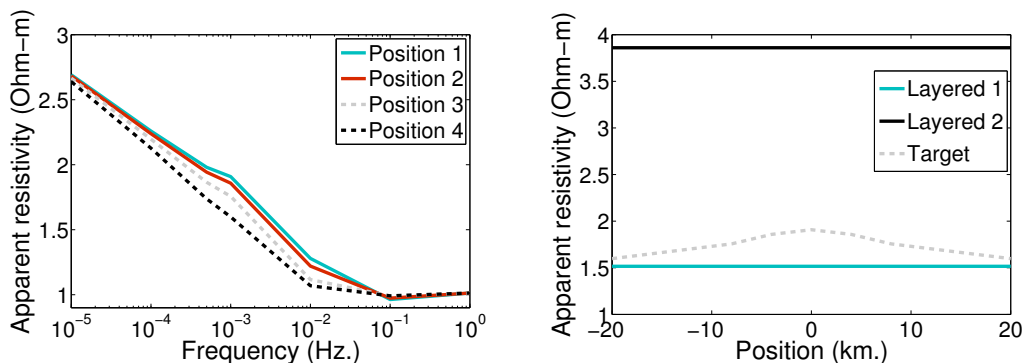


Figure 6: Left: Apparent resistivity against frequency for different positions of the receivers. Positions 1 to 4 correspond respectively to 0, 4, 8 and 20 km. of distance from the center. Right: Apparent resistivity at different distances for three different subsurface formations.

	ρ_1	ρ_2	ρ_3	ρ_4
Layered 1	1	2	3	-
Layered 2	1	10	3	-
Target	1	2	3	10

Table 2: Different models of the formation of the subsurface. The resistivity is given in Ohm-m.

5 Conclusions

To find an equilibrium between a fast and a slow decay on the PML region is usually tricky. It depends on the problem itself and it is even more complicated when there exists high contrasts on adjacent material properties. We have shown that in these complicated scenarios, the Automatically Adapted PML provides an adequate decay, not so fast to require a too fine grid and not so slow to introduce artificial reflections.

We have shown that once the decay in the PML is defined, the PML parameters are automatically tuned without any additional user interaction according to the layer widths, providing accurate solutions for the MT problem.

References

- [1] J. Alvarez-Aramberri, D. Pardo, and H. Barucq. Inversion of magnetotelluric measurements using multigoal oriented hp-adaptivity. *Procedia Computer Science*, 18:1564–1573, 2013.
- [2] J-P. Berenger. A perfectly matched layer for the absorption of electromagnetic waves. *Journal of computational physics*, 114(2):185–200, 1994.
- [3] A. Bermúdez, L. Hervella-Nieto, A. Prieto, and R. Rodríguez. Perfectly matched layers for time-harmonic second order elliptic problems. *Archives of Computational Methods in Engineering*, 17(1):77–107, 2010.
- [4] L. Cagniard. Basic theory of the magneto-telluric method of geophysical prospecting. *Geophysics*, 18(3):605–635, 1953.
- [5] W.C. Chew and W. H. Weedon. A 3d perfectly matched medium from modified maxwell’s equations with stretched coordinates. *Microwave and optical technology letters*, 7(13):599–604, 1994.
- [6] L. Demkowicz. *Computing with hp-adaptive Finite Elements: Volume 1 One and Two Dimensional Elliptic and Maxwell Problems*, volume 1. Chapman and Hall/CRC, 2006.
- [7] H. Grandis. An alternative algorithm for one-dimensional magnetotelluric response calculation. *Computers & Geosciences*, 25(2):119–125, 1999.
- [8] S. G Johnson. Notes on perfectly matched layers (pmls). *Lecture notes, Massachusetts Institute of Technology, Massachusetts*, 2008.
- [9] P. Joly. An elementary introduction to the construction and the analysis of perfectly matched layers for time domain wave propagation. *SeMA Journal*, 57(1):5–48, 2012.
- [10] D. Pardo. Multigoal-oriented adaptivity for hp-finite element methods. *Procedia Computer Science*, 1(1):1953–1961, 2010.
- [11] D. Pardo, L. Demkowicz, C. Torres-Verdin, and M. Paszynski. A self-adaptive goal-oriented hp-finite element method with electromagnetic applications. part ii: Electrodynamics. *Computer methods in applied mechanics and engineering*, 196(37-40):3585–3597, 2007.
- [12] D. Pardo, L. Demkowicz, C. Torres-Verdín, and L. Tabarovsky. A goal-oriented hp-adaptive finite element method with electromagnetic applications. part i: electrostatics. *International Journal for Numerical Methods in Engineering*, 65(8):1269–1309, 2006.
- [13] J. Pedersen and J. F. Hermance. Least squares inversion of one-dimensional magnetotelluric data: An assessment of procedures employed by brown university. *Surveys in Geophysics*, 8(2):187–231, 1986.
- [14] F. Simpson and K. Bahr. *Practical magnetotellurics*. Cambridge University Press, 2005.
- [15] F.L. Teixeira and W.C. Chew. Pml-fdtd in cylindrical and spherical grids. *Microwave and Guided Wave Letters, IEEE*, 7(9):285–287, 1997.
- [16] F.L. Teixeira and W.C. Chew. Analytical derivation of a conformal perfectly matched absorber for electromagnetic waves. *Microwave and Optical technology letters*, 17(4):231–236, 1998.
- [17] K. Vozoff. The magnetotelluric method in the exploration of sedimentary basins. *Geophysics*, 37(1):98–141, 1972.
- [18] K. Vozoff. Magnetotellurics: Principles and practice. *Proceedings of the Indian Academy of Sciences-Earth and Planetary Sciences*, 99(4):441–471, 1990.
- [19] A.J. Ward and J.B. Pendry. Calculating photonic greens functions using a nonorthogonal finite-difference time-domain method. *Physical Review B*, 58(11):7252, 1998.